Clays and Clay Minerals, Vol. 48, No. 6, 655–664, 2000.

PEDOGENIC SMECTITES IN PODZOLS FROM CENTRAL FINLAND: AN ANALYTICAL ELECTRON MICROSCOPY STUDY

FLORENCE GILLOT, DOMINIQUE RIGHI, AND FRANÇOISE ELSASS[1]

UMR CNRS 6532, Hydrogéologie, Argiles, Sols et Altérations, Faculté des Sciences, 86022 Poitiers Cedex, France
[1]Unité de Science du Sol, INRA, 78026 Versailles Cedex, France

Abstract—Transmission electron microscopy (TEM) including high-resolution transmission electron microscopy (HRTEM) and analytical electron microscopy (AEM) were used to study the fine clay fraction (<0.1 μm) from the eluvial E horizon of podzols located in central Finland that had developed from till materials. Soils of increasing age (6500–9850 y BP) were selected to represent a chronosequence of soil development. Expandable phyllosilicates (vermiculite, smectites) are formed in the eluvial E horizon of podzols in a short time (6500 y). TEM observations show that dissolution and physical-breakdown processes affect the clay particles. As the age of the soils increases, fragmentation and exfoliation of large precursor minerals lead to thinner clay particles of two to three layers thick. The chemical compositions of individual particles obtained by AEM indicate that expandable phyllosilicates from the E horizon of podzols are heterogeneous, involving a mixture of vermiculite, Mg-bearing smectites, and aluminous beidellite. Results suggest that heterogeneity is related to the nature of their precursors. Vermiculite and Mg-bearing smectites are derived from biotite and chlorite weathering whereas phengitic micas alter to aluminous beidellite. Because the transformation of biotite and chlorite is more rapid than phengitic micas, biotite and chlorite contributes predominantly to smectites in the younger soils, as long as ferromagnesian phyllosilicates are present in the E horizons. If not, a larger proportion of smectites is derived from phengitic micas in the older soils. Direct measurement of $d(001)$ values on lattice fringe images from alkylammonium-saturated samples shows that interlayer charge varies from high-charge expandable minerals (0.6–0.75 per half unit cell) in the younger soils to 0.5–0.6 per half unit cell in the oldest soils. Thus, the proportion of the components in the clay assemblage, as well as their chemistry and interlayer charge, change over time with soil evolution.

Key Words—Analytical Electron Microscopy, Finland, High-Resolution Transmission Electron Microscopy, Podzols, Smectites.

INTRODUCTION

Surficial deposits in Fennoscandia, central Finland, consist largely of material derived from the mechanical breakdown of unweathered rocks and preglacial sediments during the last glaciation. After deglaciation, large areas were submerged, but in the course of uplift, land was gradually uncovered. As a consequence, the duration of pedogenesis was confined to the post-glacial period giving rise to soils that have undergone various times of formation, with podzolization being the major soil-forming process. Because the ages of these soils are approximately known, these soils are suitable to evaluate the effect of time on clay-mineral transformations in podzols of increasing age (6500–10,000 y BP) developed from sandy tills. Previous studies described clay-mineral transformations in similar chronosequences of podzols from Finland.

Podzolization induces strong alteration of soil-clay minerals leading to the formation of smectite clay (Gjems, 1967; Righi *et al.*, 1988). Previous investigations showed that expandable minerals are present only in the eluvial E horizon of the podzols. Thus, we chose to study this material to understand genesis of expandable clays. X-ray diffraction analysis (Gillot, 1999; Gillot *et al.*, 1999; Righi *et al.*, 1997) showed that smectites and illite-smectite interstratifications are the dominant clay minerals in the E horizons of soils older than 6500 y BP. The amount of interstratified minerals decreases with evolution of the soil, producing a nearly pure smectite phase in the oldest soil (9850 y). The smectites are beidellitic, exhibiting a tetrahedral charge. Moreover, smectite of low-charge and high-charge layers is present in the samples, but low-charge smectite layers were found only in the two older soils (9550–9850 y).

The purpose of this work was to understand the origin of the various populations of these pedogenic smectites by investigating the structure and crystal chemistry of individual clay particles. Investigations were made using transmission electron microscopy (TEM) that includes high-resolution transmission electron microscopy (HRTEM) and analytical electron microscopy (AEM). As shown by Aoudjit *et al.* (1995, 1996), TEM and AEM are essential analytical methods to obtain detailed information on clay-formation processes on these heterogeneous systems.

Weathering of primary minerals in forest ecosystems is the most important natural long-term proton sink that counteracts soil acidification and base-cation depletion. Because micas and chlorites release Mg and K, they play a major role in this process. The mech-

Copyright © 2000, The Clay Minerals Society

https://doi.org/10.1346/CCMN.2000.0480607 Published online by Cambridge University Press

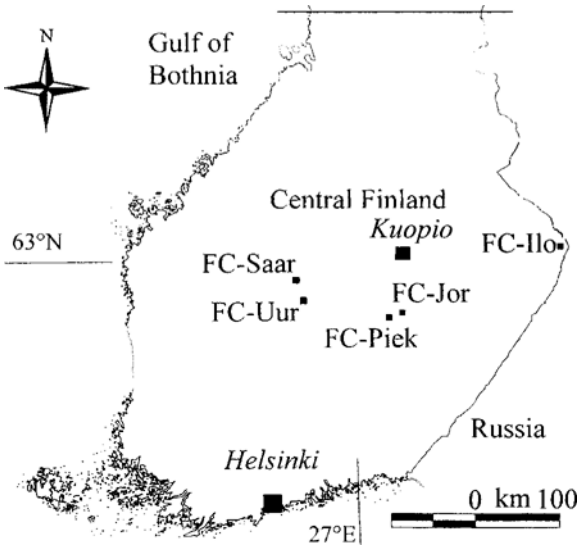


Figure 1. Sampling sites in Finland.

anisms and rates at which micas and chlorite weather are therefore critical to assess soil fertility and to predict long-term stability of forest ecosystems.

MATERIALS AND METHODS

The fine clay fraction (<0.1 μm) from the eluvial E horizon of five podzols from central Finland was selected for this study. They are the same samples as examined by Righi *et al.* (1997). The soils were selected along an east to west transect (Figure 1) to minimize differences in soil evolution that could be attributed to the north to south climatic gradient. Vegetation is Norway spruce, except for the oldest site where Scotch pine is also present (Table 1). Parent materials are sandy or stony sandy tills derived from granitic and granodioritic rocks. Homogeneity of the parent materials in the selected soils was evaluated by estimating the mineralogical distributions in the <2-mm samples. Based on these distributions, parent till materials do not exhibit large heterogeneity over the whole sequence (Righi *et al.*, 1997). All the selected soils are Podzosols according to the Référentiel Pédologique (INRA, 1995) or Typic Haplocryods according to USDA Soil Taxonomy. They exhibit a clear light-gray or pinkish-gray E horizon, 5–10 cm thick. The E horizons overlay thin (2–5 cm), discontinuous, dark reddish-brown Bh horizons. The underlying Bs horizons are thicker, 15–20 cm thick, with a yellowish-red color. The C horizons (till material) occur at ~50 cm depth. Some characteristics of the selected E horizons are listed in Table 1. Soil age was evaluated from the altitude above present sea level, with reference to the age of ancient shorelines and rate of land uplift. A more detailed description of age determination is given in Righi *et al.* (1997). Soil age increases from 6500 y BP for the youngest soil FC-Jor to 9850 y BP for the oldest FC-Ilo (Table 1). The selected soils are representative of their age categories with reference to Räisänen (1996) who investigated geochemical and mineralogical properties of more than 50 podzols of 5000–9000 y in age in the Kuopio area.

The clay fractions (<2 μm) were obtained from the soil samples by sedimentation after destruction of organic matter with diluted, Na-acetate buffered H_2O_2 and dispersion at pH 9 (NaOH). After treatment with citrate-bicarbonate-dithionite (CBD) (Mehra and Jackson, 1960) to remove iron oxides and oxyhydroxides, the bulk-clay fraction was divided into fine (<0.1 μm) and coarse clay (0.1–2 μm) subfractions using a Beckman J2-21 centrifuge equipped with a JCF-Z continous-flow rotor.

Table 1. Soil site-descriptions and physicochemical data for the E horizons.

	FC-Jor	FC-Piek	FC-Uur	FC-Saar	FC-Ilo
[1]Altitude (m)	105	130	215	172	185
Soil age (y BP)	6500	8500	9500	9550	9850
Parent material	sandy till	stony sandy till	sandy till	stony sandy till	sandy till
Topographic position	moraine plateau	moraine plateau	moraine plateau	moraine terrace	moraine hill
Vegetation	Norway Spruce	Norway Spruce	Norway Spruce	Norway Spruce	Norway Spruce Scotch Pine
$pH_{(KCl)}$	4.0	3.6	4.0	3.5	3.9
[2]CEC cmol kg^{-1}	2.1	6.9	2.4	2.7	1.8
[3]O.M. g kg^{-1}	6	35	9	14	8
clay (<2 μm) g kg^{-1}	45	58	27	20	19
dominant clay minerals in the fine clay fraction (<0.1 μm)	vermiculite (smectite)	[4]hc-smectite illite-smectite (vermiculite)	hc-smectite illite-smectite	hc- and [4]lc-smectites (illite-smectite)	hc- and lc-smectites

[1] Above present sea level.
[2] CEC: cation-exchange capacity.
[3] O.M.: organic matter.
[4] hc, lc: high charge, low charge.

https://doi.org/10.1346/CCMN.2000.0480607 Published online by Cambridge University Press

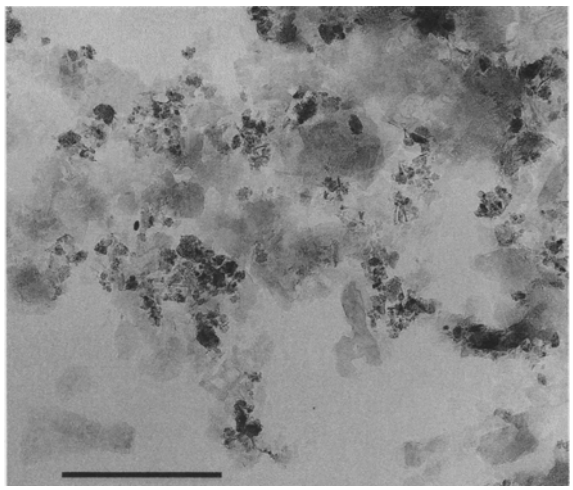


Figure 2. TEM micrograph from the fine-clay fraction of FC-Piek sample. Dark spots are Fe and/or Ti oxides. Bar: 1 μm.

Morphological observations by TEM and chemical analyses by AEM were performed on dispersed clay particles sedimented on collodion-carbon coated copper grids. A Philips 420 STEM was used at 120 kV accelerating voltage. Preset magnifications of 10,500 and 31,000 were used to obtain images of clay particles. TEM micrographs at low magnification (10,500) were also made from ultrathin sections (randomly oriented particles) prepared for HRTEM (see below). Clay textures (clay-particle size as defined by Delvaux *et al.*, 1992) were investigated on these micrographs using image-analysis software (Optilab/Optiscan). The length of particles cut perpendicular to the (001) plane was measured on the digitized image. About 400 particles were measured for each clay sample. Statistical analysis including comparison of means (least-significant difference method, rejection level 0.05) and a proportion test was made using Statistix (1998) software.

AEM was performed with a LINK AN 10000 energy dispersive system (EDS) with a windowless Si-Li detector mounted on the microscope (to detect light elements above Z = 6). Analyses were performed in transmission mode with a fixed spot (diameter 0.1 μm); analyses of smaller areas were not possible because of rapid electron-radiation damage, including element migration and mass loss. For the same reason, the acquisition time was reduced to 50 s. Results are illustrated in a ternary diagram $4Si\text{-}M^{+}\text{-}R^{2+}$ (Meunier and Velde, 1989) where M^{+} is the atomic ratio of interlayer cations (K, Na, Ca) and R^{2+} is the atomic ratio of divalent octahedral cations (only Mg in the present case, assuming Fe is in the trivalent state).

For HRTEM observations, the samples were processed using the technique of Tessier (1990). Randomly oriented pastes of fine-clay fractions coated with agar were equilibrated at 32 hPa with pure water for 24–48 h. After rehydration, water was removed with methanol, and the methanol was removed with LR White resin, a polymer of low viscosity. After polymerization of the resin at 60°C, the samples were sectioned at 50 nm by ultramicrotomy using a Reichert Ultracut E microtome. Samples saturated with K or alkylammonium (nC = 12) cations were prepared.

One-dimensional HRTEM and bright-field lattice-fringe imaging was performed on numerous crystals of each sample. The objective aperture of the microscope was fixed at 40 μm, eliminating lattice periodicities of <0.35 nm. Photographs were taken in underfocus conditions, the optimal defocus being between 100–150 nm to visualize simultaneously both 1.0 and 1.4-nm periodicities with a favorable transfer efficiency in the microscope. Zero focus was obtained on the carbon support. The preset magnification of 51,000 was used (accuracy of magnification is regularly checked with a standard mica sample).

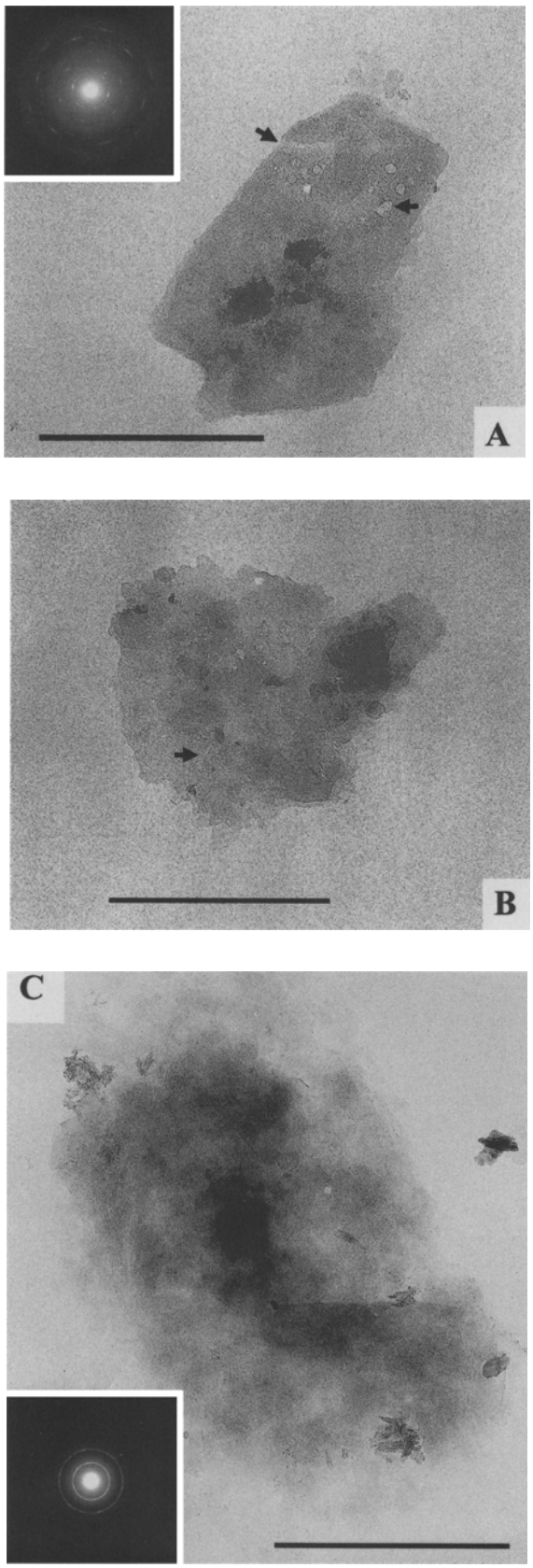
Measurements of the images were made directly from the negatives by means of a stereo-microscope equipped with a micrometric scale. Error for one measurement was estimated at 0.02 nm. The thickness and number of interlayers were measured between the centers of the two external layers, at the maximum intensity of the lattice fringe. Only stacks of layers showing strictly parallel orientation, (called "crystals" according to Tessier, 1990), either present as individual small particles or sub-units of larger quasi-crystals, were measured. At least 50 crystals were measured for each sample. Statistical analysis (comparison of means, proportion test) was made using Statistix (1998) software.

RESULTS

Morphology and texture

Similar TEM microphotographs were obtained on grain mounts of the <0.1-μm fraction of each sample. A representative low-magnification TEM micrograph shows two types of particles (Figure 2). Dark, fine-grained aggregates are Fe and/or Ti oxides (as identified by EDS). The low-contrast platy particles are phyllosilicates. The phyllosilicate particles are ~100–700 nm in size. Larger particles have sharp and straight edges and most often are found isolated. Finer particles have less distinct edges. These particles may be found separated or associated in fluffy aggregates. Observations at higher magnification show that nearly all particles exhibit dissolution features (dissolution pits), which are seen both on edges and basal faces (Figure 3A). The development of dissolution features produces particles with indented edges with a typical mosaic pattern (Figure 3B); the large particle is divided into small platelets (30–150 nm) by a discontinuous network of fine fissures. Aggregates have diffuse boundaries and are made of poorly defined small plate-

https://doi.org/10.1346/CCMN.2000.0480607 Published online by Cambridge University Press



lets giving a fluffy or cloudy pattern (Figure 3C). With the electron beam orthogonal to the (001) plane, the well defined particles produce the pseudohexagonal electron-diffraction patterns typical of ordered or semi-ordered stacking structures (Figure 3A). In contrast electron-diffraction patterns from aggregates of thin platelets display ring patterns similar to turbostratic disorder (Figure 3C), commonly observed in smectitic phyllosilicates.

Observation at low magnification of ultrathin sections shows variations in texture related to soil age. In the younger samples (FC-Jor, FC-Piek), particles are generally straight with a short lateral extension (Figure 4A). In older soils (FC-Saar, FC-Ilo), particles are longer and bent (Figure 4B). Some packets of aligned platelets (face-to-face association) exhibit a tactoid-like morphology. A change of texture with the soil age is demonstrated by measurements of particle length. The mean length (255 nm) for the older soil (FC-Ilo) is significantly different from that for the other younger soils (Table 2). The distribution of length classes is shown in Figure 5, proportions of the different classes are not significantly different from one sample to another.

HRTEM observations

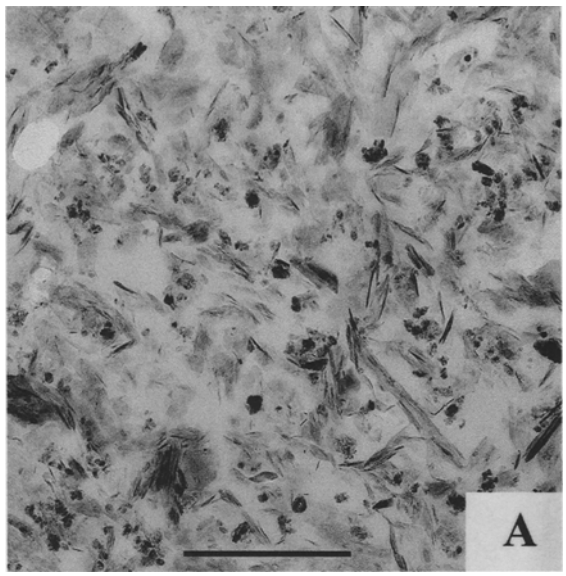
Similar TEM images are obtained from all K-saturated samples, independent of the soil age. The *d*(001) value most frequently observed is at ~1.0 nm and may be attributed to illitic crystals and to expandable phyllosilicate (vermiculite, smectite) with high interlayer charge (Figure 6A). In addition, *d*(001) values of 1.2 (Figure 6B and 6C), 1.4, and 1.6 nm (not shown) are present. The mean *d*(001) value at 1.2 nm is attributed to smectite crystals with interlayer H_2O molecules as suggested by Righi and Elsass (1996). The *d*(001) values at ~1.4 and 1.6 nm are attributed to smectite of lower charge with one (1.4 nm) or two (1.6 nm) sheets of interlayered resin molecules (Righi and Elsass, 1996). The 1.4-nm *d*(001) value is attributed also to the presence of chlorite crystals. The interplanar *d*(001) value of 1.6 nm is more abundant in the sample from the older soil FC-Ilo.

The number of layers in individual phyllosilicate crystals changes with soil age. The mean number of layers within a crystal (Table 2) varies from 4.5 (FC-Jor) to 3.2 (FC-Piek), 3.7 (FC-Uur), and 3.9 (FC-Ilo).

←

Figure 3. TEM micrographs and electron-diffraction patterns of fine-clay particles. A) FC-Saar sample, arrows show dissolution features; pseudohexagonal electron-diffraction pattern typical of ordered or semi-ordered stacking structures; B) FC-Saar sample, mosaic pattern, arrow shows microfissure; C) FC-Ilo sample, fluffy aggregate pattern; ring electron-diffraction pattern similar to turbostratic disorder. Bar: 500 nm.

https://doi.org/10.1346/CCMN.2000.0480607 Published online by Cambridge University Press



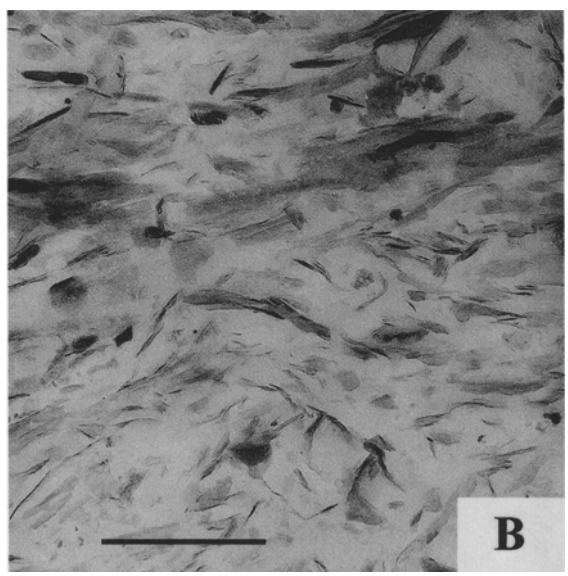


Figure 4. TEM micrograph (low magnification) of ultrathin section of fine-clay particles. A) FC-Piek sample; B) FC-Ilo sample. Bar: 1 μm.

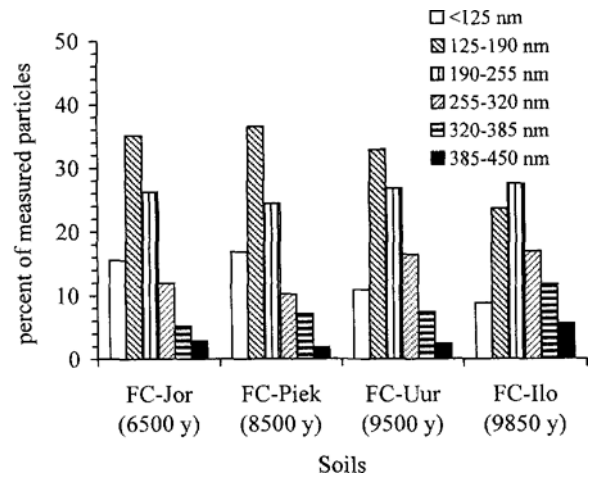


Figure 5. Histograms of length classes of fine-clay particles from four E horizons.

There are three groups where the means are not significantly different, the first group contains only sample FC-Jor, the second group contains samples FC-Piek and FC-Uur, and the third group contains samples FC-Uur and FC-Ilo. Figure 7 shows the frequency distribution of layers in the five samples. The FC-Jor sample contains crystals from all frequency classes. Compared to the other samples, the FC-Piek sample, the next oldest after sample FC-Jor, is characterized by a significantly greater frequency of crystals with only two or three layers. Note that crystals with six or more layers are nearly absent in this sample. In addition, many single-layer particles are observed in all samples (they are not quantified).

Lattice-fringe images from samples saturated with nC = 12 alkylammonium exhibit various mean interplanar *d*(001) values that vary with soil age (Figure 8). For the FC-Piek sample, most of the mean *d* values are distributed in the 2.11–2.30, 2.31–2.50, and >2.51 nm classes, which indicate pseudo-trilayers and paraffin-like arrangements (>2.51 nm) of the alkylammonium chains. According to Olis *et al.* (1990), such mean *d*(001) values correspond to mean interlayer charges of 0.60–0.70, 0.70–0.75, and >0.75 per half unit cell, respectively. For the FC-Ilo sample, a mean *d*(001) value of 1.91–2.10 nm is observed, which in-

Table 2. Mean length and number of layers of clay particles from the <0.1-μm fraction of E horizons.

Sample		FC-Jor	FC-Piek	FC-Uur	FC-Ilo
soil age (y BP)		6500	8500	9500	9850
mean length (nm)	length [1](SD)	207 (89)	204 (96)	224 (90)	255 (130)
homogeneous groups		[2]a	a	a	[2]b
mean number of layers	layers (SD)	4.5 (1.9)	3.2 (1.1)	3.7 (1.4)	3.9 (1.0)
homogeneous groups		a	b	b, [2]c	c

[1] (SD): standard deviation.
[2] a, b, c: same letter indicates samples for which the means are not significantly different.

https://doi.org/10.1346/CCMN.2000.0480607 Published online by Cambridge University Press

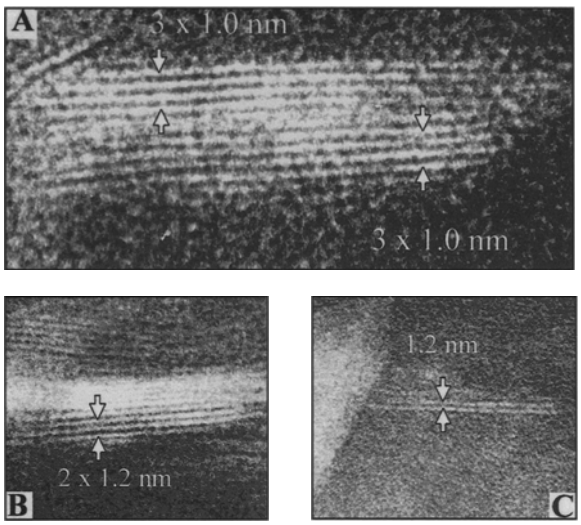


Figure 6. Lattice-fringe images of fine clay from FC-Ilo sample. A) delimited by arrows, two crystals with three interlayers [$d(001)$ = 1.0 nm]; B) delimited by arrows, crystal with two interlayers [$d(001)$ = 1.2 nm]; C) delimited by arrows, two-layer crystal [$d(001)$ = 1.2 nm].

dicates interstratification of bilayer and pseudo-trilayer arrangements and a mean interlayer charge of 0.5–0.6 per half unit cell. The proportion of this population of expandable phyllosilicates with a lower charge is significantly greater in the older FC-Ilo sample than in the FC-Piek sample.

Analysis of individual particles by AEM

Compositional data from AEM of <0.1-μm clay particles from the E horizon are plotted in a ternary diagram 4Si-R^{2+}-M^{+}. Such a diagram (Figure 9) displays chemical-composition fields of common phyllosilicates found in soils (muscovite, phengite, biotite, chlorite, vermiculite, smectite) on the basis of their Si content (4Si), octahedral composition (R^{2+}), and layer charge (M^{+}). The chemical-composition field for soil vermiculites is obtained from analyses by Douglas (1989, p. 643–645). The AEM-determined composi-

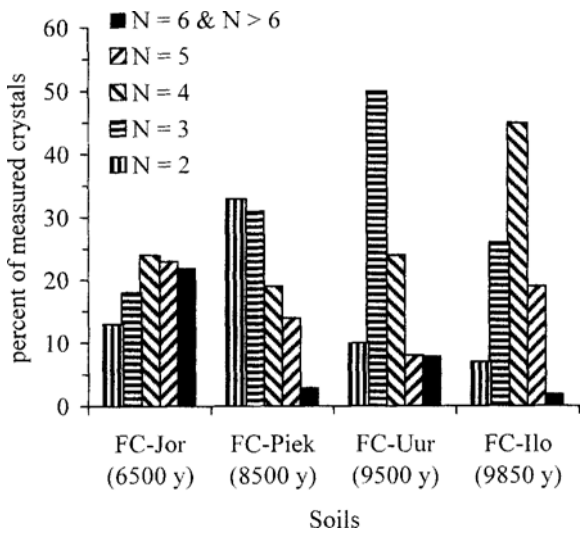
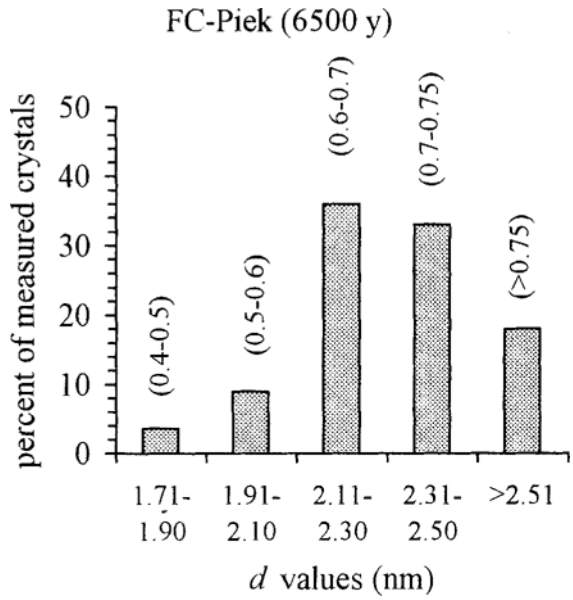


Figure 7. Histograms of number of layers (N) by crystal of fine clays from four E horizons.



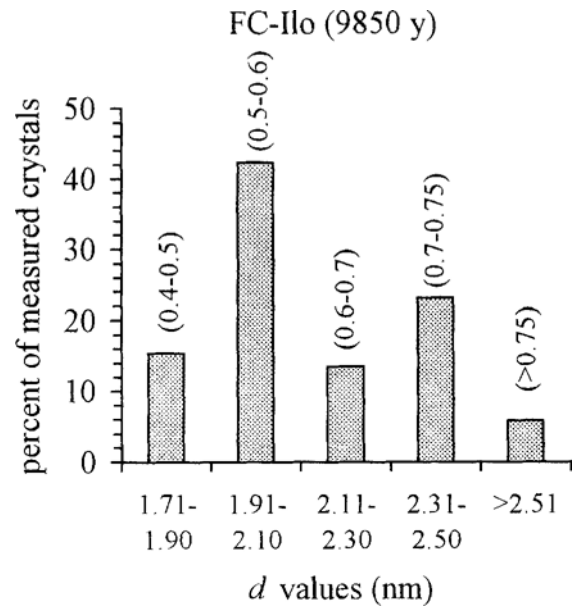


Figure 8. Histograms of $d(001)$ values (nm) measured on lattice-fringe images from fine-clay samples. Clays are saturated with nC = 12 alkylammonium ions. Values within brackets are interlayer charges (per half unit cell) calculated from the corresponding $d(001)$ values.

https://doi.org/10.1346/CCMN.2000.0480607 Published online by Cambridge University Press

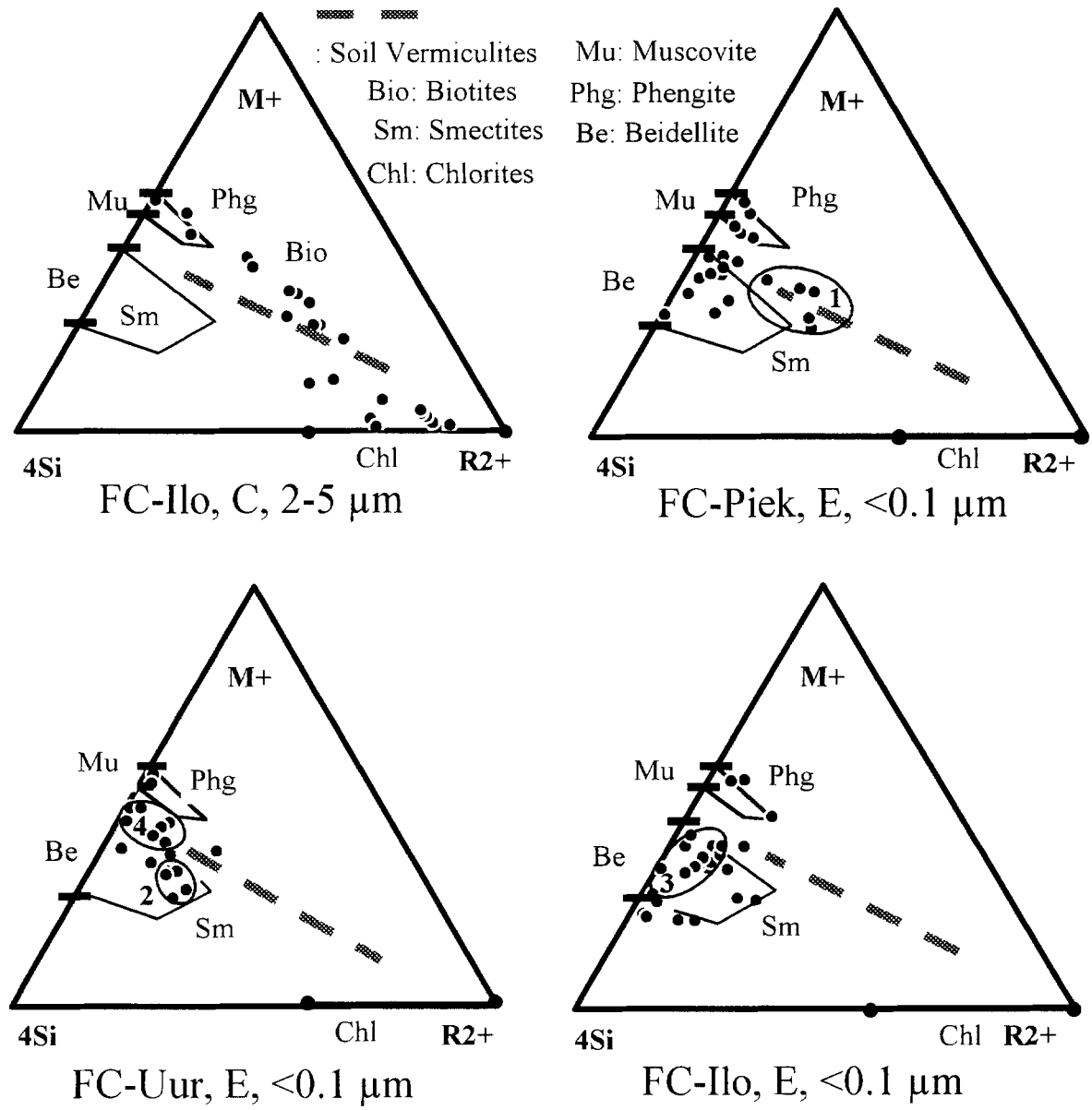


Figure 9. Plots of chemical composition of individual particles in triangular M^{+}-4Si-R^{2+} diagrams. AEM analyses. C and E are for C (till material) and E horizons, 2–5 and <0.1 μm indicate the grain fraction analyzed. See text for explanation.

tions of larger fine-silt particles (2–5 μm) from the C horizons were also analyzed to obtain information on phyllosilicates that are potential parent minerals for the soil-clay fraction (Figure 9). Analyzed phyllosilicates in samples of the C horizon have chemical compositions that are distributed between the composition fields of chlorite, biotite, vermiculite, and phengite.

Compared to that of the fine-silt particles from the C horizons, the chemical compositions of fine clay particles from the E horizons are greatly changed. Particles with a chlorite or biotite chemical composition are absent. A few particles from the FC-Piek sample are found with a chemical composition of soil vermiculites (Figure 9, field 1), particles with such composition are not present in samples from the older soils FC-Uur and FC-Ilo (Figure 9). The chemical composition of clays of these oldest two samples plot in the compositional field of smectites. The bulk of particles with smectite chemical composition may be further divided into two groups. One chemical composition (Figure 9, field 2) is near ideal montmorillonite, because this group is Si-rich and contains Mg. The second group (Figure 9, field 3) includes particles containing only limited Mg and the particles have chem-

https://doi.org/10.1346/CCMN.2000.0480607 Published online by Cambridge University Press

ical compositions close to that of beidellite. Particles from this latter group are the most common in the FC-Ilo sample. In addition, particles with chemical composition intermediate between phengite and smectites (Figure 9, field 4) are found in the FC-Piek and FC-Uur samples, but not in the sample from the older soil FC-Ilo.

The composition of individual particles as determined by AEM shows that smectites from the E horizons are heterogeneous. However, the data indicate a decrease of the number of particles of soil vermiculite (Figure 9, field 1) or of Mg-bearing smectite composition (Figure 9, field 2) with soil age.

DISCUSSION

Podzolization is the major pedogenetic process which affects till materials in central Finland. In this system, soil-clay minerals are produced essentially by weathering of primary phyllosilicates, particularly micas and chlorite. Previous authors established that in the eluvial E horizon of podzols, expandable phyllosilicates (vermiculite, smectite) are formed (Gjems, 1963; Kodama and Brydon, 1968; Ross *et al.*, 1982; McDaniel *et al.*, 1995). Processes leading to the formation of smectite clay from preexisting phyllosilicates involve physical breakdown and chemical alteration.

Texture and alteration

TEM observations showed that dissolution processes produce the fragmentation of large particles into smaller remnants, which involve mosaic-like platelets and poorly shaped aggregates. This process also induces structural change. Ordered layer stackings, being characteristic of primary phyllosilicates, change to disordered turbostratic-like stacking in the strongly weathered products. Wilson (1987) describes podzol smectites as morphologically similar to vermiculite, yielding a "single-spot" type of electron diffraction pattern. These types of particles are found in the studied podzols, but also particles occur with a lower degree of stacking order between the layers that produce the typical ring diffraction pattern observed for smectites.

Physical breakdown appears to produce clay particles of various shape and size. In the younger soils, a population of rather short and thick particles dominates the clay assemblage. Aoudjit *et al.* (1996) and Hardy *et al.* (1999) describe such particles. They are short (<200 nm) and thick with respect to their length, as typically produced by the physical breakdown of biotites and chlorites. The greater proportion of relatively thin and flexible particles observed in older soils is attributed either to a more advanced stage of weathering related to the soil age or to the presence of precursor minerals other than biotite or chlorite. Phengitic micas, present in the parent materials, are a possible source of these particles. Phengitic micas are less susceptible to weathering than biotite or chlorite, and are expected to be present in larger proportion as the time for pedogenesis increases. Breakdown of phentgitic micas will produce clay minerals at later stages of pedogenesis with different compositions.

Crystal thickness, determined by the number of layers in a crystal, varies from one sample to another. Except for the youngest sample FC-Jor, crystals with six or more layers constitute only a very small portion of the fine clays. Moreover, for the FC-Piek sample (the next oldest after FC-Jor) a large proportion of two-layer crystals is present. This suggests that thick crystals (number of layers >6) present in the younger soils are transformed through an intensive exfolation process to produce thinner crystals in the older soils. The strong decrease of the relative amount of thick crystals would also indicate that, as time involving pedogenesis increases, thick exfoliated crystals are not replaced by new crystals from the fragmentation of precursors of a larger size. The fact that they are not replaced is explained by the impoverishment in large precursor minerals as pedogenesis progresses. Assuming that thick particles derive from the physical breakdown of chloritic or biotitic minerals, this is consistent with the expected rapid weathering of biotites and chlorites in soils subjected to podzolization. The proportion of two-layer crystals, which is the greater in the FC-Piek sample, strongly decreases in the two older samples FC-Uur and FC-Ilo. This suggests a preferential dissolution of the thinner crystals and the relative concentration of thicker crystals.

Geochemical alteration

The fields of chemical compositions obtained from samples of soils of increasing age suggest a general trend of chemical alteration by clay particles during pedogenesis. The major processes involved are a loss of octahedral Fe and Mg, a decrease of the total layer charge, and a decrease of Si for Al tetrahedral site substitutions. Such processes occur in the transformation of mica or chlorite to expansible 2:1 phyllosilicates (Douglas, 1989; Proust *et al.*, 1986).

Chemical analyses of individual clay particles show that smectites from the E horizons of podzols are chemically heterogeneous, covering a rather wide range of chemical compositions. The chemical compositions displayed in Figure 9 suggest the formation of smectitic clay particles through the transformation of two different types of precursor minerals. A few particles with soil-vermiculite composition (Figure 9, field 1) are present in the FC-Piek sample. Conversely, chloritic and biotitic particles, well represented in the parent material, are not found in the FC-Piek sample, suggesting the pedogenic dissolution and/or transformation of mica and chlorite minerals to produce soil vermiculite. The particles with soil-vermiculite com-

https://doi.org/10.1346/CCMN.2000.0480607 Published online by Cambridge University Press

position are not found in the samples from older soils (FC-Uur and FC-Ilo). Instead, particles with a smectite composition containing Mg (Figure 9, field 2) are present in these samples. This suggests that vermiculite (Figure 9, field 1) is altered to produce smectite (Figure 9, field 2). The transformation implies a decrease of the layer charge related to the decrease of the tetrahedral charge (increase of the 4Si relative content). The fact that smectites (Figure 9, field 2) are less abundant in the older FC-Ilo sample suggests that these smectites are progressively altered and their source minerals are depleted as pedogenesis increases.

The numerous particles with chemical composition intermediate between phengite mica and smectites (Figure 9, field 4) suggest transformation of phengitic micas to an interstratified phengitic mica and smectite phase. These interstratifications are a possible source for particles with a beidellitic chemical composition (Figure 9, field 3), which are more aluminous than the smectites (Figure 9, field 2). This is in good agreement with X-ray diffraction data (Righi *et al.*, 1997) that show mica-smectite interstratifications as an intermediate step in the formation of smectites in the studied samples. The chemical compositions of particles from older soils indicate that the smectites are primarily originating from phengite weathering. This suggests that smectites in the E horizons of podzols are formed through weathering of Fe- and Mg-rich phyllosilicates in the first stages of pedogenesis and from phengite and muscovite as pedogenesis increases.

In good agreement with X-ray diffraction results (Righi *et al.*, 1997), smectites from the E horizons of podzols include several populations with various interlayer charge. Layer-charge evaluation through measurement of d values on HRTEM images obtained from alkylammonium-saturated samples gives layer-charge values generally >0.6 per half unit cell, although a smectite behavior (swelling to 1.70 nm in ethylene glycol-solvated samples) is observed on X-ray diffraction patterns from the corresponding samples. Malla and Douglas (1987) observed similar behavior in soil clays with two sheets of an ethylene glycol complex in clays with layer charge as high as 0.72 per half unit cell.

Smectites with a lower charge were only observed in the fine-clay fraction (<0.1 μm) from the older soil FC-Ilo. This agrees with previous X-ray diffraction analysis of alkylammonium (nC = 12)-saturated fine-clay samples (Gillot, 1999) that indicated a mean interlayer charge of expandable minerals in the FC-Piek sample of ~0.73 per half unit cell, whereas expandable phyllosilicates with a mean interlayer charge of 0.70, 0.57, and 0.46 per half unit cell were found in the FC-Ilo sample.

Lower interlayer charge in smectites from older soils suggests pedogenic alteration of the high-charge smectites. Experimental alteration of smectites (Janek *et al.*, 1997) has shown that a decrease of the layer charge is easily obtained by desaturation (H^+ exchange) and "autotransformation". The effect is stronger for high-charge and/or Fe, Mg-rich smectite layers, which suggests a preferential attack by protons on the highly charged layers. Such a process would explain the alteration with time of the layer charge of the smectites of the soil chronosequence. Robert *et al.* (1979) showed that desaturation of expandable clay minerals is easily obtained by leaching with dilute solutions of weakly complexing organic acids, a situation likely to occur in these podzols.

ACKNOWLEDGMENTS

The authors thank M.L. Räisänen and collaborators from the Geological Survey of Finland for their essential support in choosing and sampling the study sites. This research was supported in part by CNRS-DRI "Programme de Recherche en Coopération sur Conventions Internationales" funds.

REFERENCES

Aoudjit, H., Robert, M., Elsass, F., and Curmi, P. (1995) Detailed study of smectite genesis in granite saprolites by analytical electron microscopy. *Clay Minerals*, **30,** 135–148.

Aoudjit, H., Elsass, F., Righi, D., and Robert, M. (1996) Mica weathering in acidic soils by analytical electron microscopy. *Clay Minerals*, **31,** 319–322.

Delvaux, B., Tessier, D., Herbillon, A.J., Burtin, G., Jaunet, A.M., and Vielvoye, L. (1992) Morphology, texture, and microstructure of halloysitic clays as related to weathering and exchangeable cation. *Clays and Clay Minerals*, **40,** 446–456.

Douglas, L.A. (1989) Vermiculites. In *Minerals in Soil Environments, 2nd edition*, J.B. Dixon and S.B. Weed, eds., Soil Science Society of America, Madison, Wisconsin, USA, 635–674.

Gillot, F. (1999) Génèse et évolution des smectites de transformation de trois chronoséquences (300–10 000 ans) de podzols de Finlande. Thesis, Université de Poitiers, Poitiers, France, 259 pp.

Gillot, F., Righi, D., and Räisänen, M.L. (1999) Formation of smectites and their alteration in two chronosequences of podzols in Finland. In *Clays to Our Future, Proceedings 11th International Clay Conference 1997*, H. Kodama, A.R. Mermut, and J.K. Torrance eds., ICC97 Organizing Committee, Ottawa, Canada, 725–731.

Gjems, O. (1963) A swelling diotahedral clay mineral of a vermiculite-smectite type in the weathering horizons of podzols. *Clay Minerals Bulletin*, **5,** 183–193.

Gjems, O. (1967) Studies on clay minerals and clay mineral formation in soil profiles in Scandinavia. *Meddelelser fra det Norske Skogforsoksvesen*, **XXI,** 303–415.

Hardy, M., Jamagne, M., Elsass, F., Robert, M., and Chesneau, D. (1999) Mineralogical development of the silt fractions of a Podzoluvisol on loess in the Paris Basin (France). *European Journal of Soil Science*, **50,** 443–456.

INRA (1995) *Référentiel Pédologique*. INRA éditions, Paris, 332 pp.

Janek, M., Komadel, P., and Lagaly, G. (1997) Effect of autotransformation on the layer charge of smectites determined by the alkylammonium method. *Clay Minerals*, **32,** 623–632.

Kodama, H. and Brydon, J.E. (1968) A study of clay minerals in podzol soils in New Brunswick, Eastern Canada. *Clay Minerals*, **7,** 295–309.

https://doi.org/10.1346/CCMN.2000.0480607 Published online by Cambridge University Press

Malla, P.B. and Douglas, L.A. (1987) Identification of expending layer silicates: Layer charge vs. expension properties. In *Proceedings of the International Clay Conference, Denver, 1985*, L.G. Schultz, H. van Olphen, and F.A. Mumpton, eds., The Clay Mineral Society, Bloomington, Indiana, 227–283.

McDaniel, P.A., Falen, A.L., Tice, K.R., Graham, R.C., and Fendorf, S.E. (1995) Beidellite in E horizons of northern Idaho Spodosols formed in volcanic ash. *Clays and Clay Minerals*, **43,** 525–532.

Mehra, O. and Jackson, M.L. (1960) Iron oxide removal from soils and clays by dithionite-citrate system buffered with sodium bicarbonate. *Clays and Clay Minerals*, **7,** 317–327.

Meunier, A. and Velde, B. (1989) Solid solutions in I/S mixed layer minerals and illite. *American Mineralogist*, **74,** 1106–1112.

Olis, A.C., Malla, P.B., and Douglas, L.A. (1990) The rapid estimation of the layer charge of 2:1 expanding clays from a single alkylammonium ion expansion. *Clay Minerals*, **25,** 39–50.

Proust, D., Eymery, J.P., and Beaufort, D. (1986) Supergene vermiculitization of magnesian chlorite: Iron and magnesium removal process. *Clays and Clay Minerals*, **34,** 572–580.

Räisänen, M.L. (1996) *Geochemistry of Podzolized Tills and the Implications for Aluminium Mobility Near Industrial Sites: A Study in Kuopio, Eastern Finland.* Geological Survey of Finland, Bulletin 387, Espoo, 72 pp.

Righi, D. and Elsass, F. (1996) Characterization of soil clay minerals: Decomposition of X-ray diffraction diagrams and high resolution electron microscopy. *Clays and Clay Minerals*, **44,** 791–800.

Righi, D., Ranger, J., and Robert, M. (1988) Clay minerals as indicators of some soil forming processes in the temperate zone. *Bulletin de Minéralogie*, **111,** 625–632.

Righi, D., Räisänen, M.L., and Gillot, F. (1997) Clay mineral transformations in podzolized tills in central Finland. *Clay Minerals*, **32,** 531–544.

Robert, M., Razzaghe-Karimi, M.H., Vicente, M.A., and Veneau, G. (1979) Rôle du facteur biochimique dans l'altération des minéraux silicatés. *Science du Sol*, **2–3,** 153–174.

Ross, G.J., Wang, C., Ozkan, A.I., and Rees, H.W. (1982) Weathering of chlorite and mica in a New Brunswick podzol developed on till derived from chlorite-mica schist. *Geoderma*, **27,** 255–267.

Tessier, D. (1990) Behaviour and microstructure of clay minerals. In *Soil Colloids and Their Associations in Aggregates*, M.F. De Boodt, M. Hayes, and A. Herbillon, eds., Plenum Publishing Corporation, New York, USA, 387–414.

Wilson, M.J. (1987) Soil smectites and related interstratified minerals: Recent devolpments. In *Proceedings of the International Clay Conference, Denver, 1985*, L.G. Schultz, H. van Olphen, and F.A. Mumpton, eds., The Clay Minerals Society, Bloomington, Indiana, 167–173.

E-mail of corresponding author: dominique.righi@hydrasa.univ-poitiers.fr

(Received 14 January 2000; accepted 1 July 2000; Ms. 420; A.E. Peter J. Heaney)

https://doi.org/10.1346/CCMN.2000.0480607 Published online by Cambridge University Press